2011 American Control Conference
on O'Farrell Street, San Francisco, CA, USA
June 29 - July 01, 2011

Model Predictive Control for Spacecraft Rendezvous and Docking with a Rotating/Tumbling Platform and for Debris Avoidance

Hyeongjun Park, Stefano Di Cairano and Ilya Kolmanovsky

***Abstract*— A Model Predictive Control (MPC) approach is developed for spacecraft rendezvous and docking to a rotating/tumbling platform and for debris avoidance maneuvers. With this approach, the constraints on thrust, approach velocity and spacecraft positioning within the Line-of-Sight cone from the docking port are systematically treated. The trajectories are simulated and time-to-dock and fuel consumption are evaluated as cost function parameters are varied. Debris avoidance maneuvers are considered, with the debris in the spacecraft rendezvous path.**

I. Introduction

Rendezvous and proximity maneuvers are important parts of spacecraft missions, which may be necessary to recover a tumbling/out-of-control satellite, that may exhibit complicate motion, or to avoid debris appearing on the rendezvous path. The requirements in rendezvous and docking problems lead to control problems with imposed pointwise-in-time and terminal constraints on both state and control variables. For instance, the approaching spacecraft must maintain its position within a Line-of-Sight (LOS) cone from the docking port on the target platform. In addition, terminal velocity of the spacecraft should match the velocity of the docking port to ensure soft-docking. Collision with debris on the spacecraft path must be avoided, and the spacecraft fuel consumption must be minimized during the maneuvers.

The above requirements and constraints can be systematically treated using a Model Predictive Control (MPC) framework. As an example, we consider an application of this framework to spacecraft docking and debris avoidance maneuvers in orbital plane. The target platform is disk-shaped, and is assumed to rotate with constant angular velocity around its center of mass.

The rendezvous and docking problems have been studied in the literature, see, e.g., [1], [2] and the references therein. Prior work on applying MPC to spacecraft rendezvous and docking includes [4], where auxiliary integer variables are introduced to represent the state of the mission at a given time (specifically whether a prescribed "box" around the docking port is reached or yet to be reached) and the problem is treated as a mixed integer programming problem where the objective function is the weighted sum of fuel consumption and maneuver time. Recent publications on the application of MPC to these problems also include [6], [7].

Hyeongjun Park and Ilya Kolmanovsky are with Department of Aerospace Engineering, University of Michigan, Ann Arbor, MI 48109, USA judepark@umich.edu, ilya@umich.edu,

Stefano Di Cairano is with Powertrain Control R&A, Ford Motor Company, Dearborn, MI 48124, USA sdicaira@ford.com

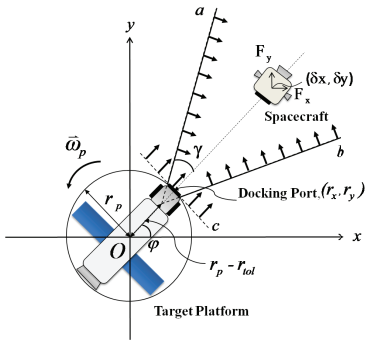

Fig. 1. Spacecraft and a target platform.

In this paper, we treat the problem using a computationally more tractable linear-quadratic MPC formulation, where the cost penalizes the control effort and distance to the docking port. In the formulation proposed here, all the variables are real-valued so that the resulting optimization problem is a quadratic program, where complexity is polynomial as opposed to exponential complexity of integer programs. We also impose LOS constraints and demonstrate that the soft-docking constraints can be enforced by replacing them by appropriately defined, convex, pointwise-in-time constraints. Compared to our previous work [3], where a non-rotating platform is considered, here we demonstrate that prediction of the platform and docking port motion, in the case of a rotating platform, is beneficial in terms of being able to satisfactorily complete a larger variety of maneuvers and in terms of reducing fuel consumption. Furthermore, by introducing virtual rotating platforms around debris, debris avoidance maneuvers can be performed.

In the rest of the paper, in Section II we recall the dynamical model used for describing the motion of the spacecraft relative to the platform, and in Section III we discuss the MPC control design for the case of a rotating platform. In Section IV we present the results in several simulated maneuvers. The proposed approach is applied to the debris avoidance in Section V and the conclusions are summarized in Section VI.

II. Problem Formulation

We consider an autonomous rendezvous between a spacecraft and a target platform. The platform has disk shape of radius r_p, and rotates at a constant angular velocity ω_p (see Fig. 1). The target platform is in a circular orbit around the Earth, with orbit radius R_0, and the spacecraft motion is confined to the orbital plane.

978-1-4577-0079-8/11/$26.00 ©2011 AACC

The linearized continuous-time dynamical model for the rendezvous problem has the form [8]

$$\dot{X} = AX + BU, \tag{1}$$

where $X = (\delta x\ \delta y\ \delta\dot{x}\ \delta\dot{y})^T$, $U = (u_x\ u_y)^T$, and

$$A = \begin{pmatrix} 0 & 0 & 1 & 0 \\ 0 & 0 & 0 & 1 \\ 3n^2 & 0 & 0 & 2n \\ 0 & 0 & -2n & 0 \end{pmatrix}, B = \begin{pmatrix} 0 & 0 \\ 0 & 0 \\ 1 & 0 \\ 0 & 1 \end{pmatrix}.$$

Here, δx and δy are components of the position of the spacecraft relative to the center of the platform, u_x and u_y are the acceleration components of the spacecraft induced by the thrusters in the x and y directions, respectively, and n is the target platform orbital rate, $n = \sqrt{\mu/R_0^3}$, where μ is the gravitational constant. The disturbances due to air drag, solar pressure and non-ideal gravity perturbations are neglected in the model formulation as the effects of these disturbances during the short time period of the maneuver can be easily compensated by the MPC. In the case of impulsive thrusters, we assume that the commanded thrust force magnitude and direction are realized by appropriate thruster on-off times [2].

The spacecraft must approach the port while remaining within a Line-of-Sight (LOS) cone from the port. A soft-docking constraint is imposed so that the velocity of the spacecraft once it reaches the port is close to the velocity of the platform. Since the platform has convex shape, by remaining within a Line-of-Sight cone and by matching the velocity of the port, the spacecraft is guaranteed not to collide with the platform. A debris avoidance constraints will also be introduced and treated later in the paper.

III. Model Predictive Control Design

We now proceed with deriving a discrete-time model, approximating the constraints, and designing the MPC controller. By sampling (1) with period T_s, a discrete-time model for the spacecraft motion relative to the platform is obtained

$$X(k+1) = A_d X(k) + B_d U(k) \tag{2}$$

where $X(k)$ and $U(k)$ are state and input vectors at the sampling instant k. In order to define the cost function for the MPC controller, we compute first the value function of the infinite horizon unconstrained LQ problem for stabilizing the relative position and velocity of the spacecraft to the origin,

$$\min_{\{U(k)\}_{k=0}^{\infty}} J = \sum_{k=0}^{\infty} X(k)^T Q X(k) + U(k)^T R U(k) \tag{3}$$

where, Q, R, are positive definite diagonal matrices. Let P be the solution of the Riccati equation resulting in the value function $\mathcal{V}(X(0)) = X(0)^T P X(0)$ for the LQ problem. We use P in the terminal cost of the MPC problem as a stability enforcing mechanism.

For the formulation and treatment of the MPC problem where the platform is rotating, additional state variables r_x, r_y, σ_x and σ_y are introduced, where $r_x(k)$ and $r_y(k)$ identify the coordinates of the docking port at the time instant k and $\sigma_x(k)$ and $\sigma_y(k)$ are relative coordinates of the spacecraft with respect to the docking port at the time instant k. Due to platform rotation,

$$\begin{aligned} r_x(k+1) &= \cos(\omega_p T_s) r_x(k) - \sin(\omega_p T_s) r_y(k), \\ r_y(k+1) &= \sin(\omega_p T_s) r_x(k) + \cos(\omega_p T_s) r_y(k), \end{aligned} \tag{4}$$

$$\begin{aligned} \sigma_x(k+1) &= \delta x(k) - r_x(k), \\ \sigma_y(k+1) &= \delta y(k) - r_y(k). \end{aligned} \tag{5}$$

From (2), (4), (5), by defining the augmented state vector as

$$\bar{X} = \left(\delta x\ \delta y\ \delta\dot{x}\ \delta\dot{y}\ r_x\ r_y\ \sigma_x\ \sigma_y \right)^T,$$

the model can be written in the form,

$$\bar{X}(k+1) = \bar{A}\bar{X}(k) + \bar{B}\bar{U}(k) \tag{6}$$

with appropriately defined $\bar{A}$ and $\bar{B}$, $\bar{U} = [U^T\ s]^T$, where s is an auxiliary variable used in the definition of the constraints, as explained next.

Due to physical limits of the trusters we need to enforce at any time instant k the control constraints

$$U_{\min} \leq U(k) \leq U_{max}. \tag{7}$$

Next, we define the system constraints based on the specifications of soft-docking and LOS constraints. The soft-docking constraint ensures that the velocity of the spacecraft, when approaching the docking port, converges to the docking port velocity. To handle this terminal constraint, we first replace it by a related pointwise-in-time constraint, requiring that the 1-norm of the spacecraft velocity relative to the docking port is bounded by an affine function of the 1-norm of the distance of the spacecraft relative to the docking port. This approach is a generalization to the multi-dimensional context of the approach used in [5] to treat a soft-landing constraint for an electromagnetic actuator. Specifically, the following constraint is imposed over the prediction horizon in the MPC problem

$$\begin{aligned} \zeta(k) &\stackrel{\Delta}{=} |\sigma_x(k)| + |\sigma_y(k)| \\ &\geq \eta(|\delta\dot{x}(k) - v_{p_x}(k)| + |\delta\dot{y}(k) - v_{p_y}(k)| - s(k)) - \beta, \end{aligned} \tag{8}$$

where v_{p_x} and v_{p_y} are velocity components of the docking port. The port velocities can be computed as $v_{p_x}(k) = -\omega_p r_y(k)$ and $v_{p_y}(k) = \omega_p r_x(k)$. The values $\eta > 0$ and $\beta > 0$ are constant parameters and $s(k)$ is a slack variable, which is introduced to avoid infeasibility of the constraint. Constraint (8) is nonlinear, and in order to handle it in a linear-quadratic MPC approach it needs to be formulated as a linear constraint. We do this assuming that along the constraint horizon the signs of $\delta\dot{x}(k) - v_{p_x}(k)$ and $\delta\dot{y}(k) - v_{p_y}(k)$ does not change. Thus, we enforce

$$\Phi_x(k)\bar{X}(k) + \Phi_u\bar{U}(k) \geq -\beta \tag{9}$$

where $\Phi_x(k) = \left[0\ 0\ -\psi_1(k)\ -\omega_p\psi_1(k)\ \psi_2(k)\ -\omega_p\psi_2(k) \right]$, $\psi_1 = \eta \mathrm{sgn}(\dot{x}(k) - v_{p_x}(k))$, $\psi_2 = \eta \mathrm{sgn}(\dot{y}(k) - v_{p_y}(k))$, and sgn is the sign function, $\Phi_u = \left[0\ 0\ \eta \right]$.

Besides the soft-docking constraints, the spacecraft trajectory must satisfy the LOS constraints which confine the

spacecraft to the intersection of the LOS cone, with vertex moved slightly inside the platform, and a half-plane, see **a**, **b**, **c** in Fig. 1. Let γ denote the half of the LOS cone angle and let r_{tol} denote the distance by which the vertex of LOS cone is moved inside the platform. The value $r_{tol} > 0$ slightly relaxes the LOS constraints to facilitate the application of MPC and mitigate ill-conditioning of the problem caused by cone constraints becoming almost infeasible when the docking port is approached (as **a** and **b** come arbitrary close together and the platform rotates). The half-plane constraint **c** is defined by the tangent line to the platform at the position of the docking port, and it ensures that collisions of the spacecraft with the target platform are avoided even with the relaxed LOS cone constraints.

The LOS constraints are described by

$$\begin{aligned}
\textbf{a}\text{:}\quad & \frac{\sin(\varphi(k)+\gamma)}{(r_p-r_{tol})\sin\gamma}\delta x(k) - \frac{\cos(\varphi(k)+\gamma)}{(r_p-r_{tol})\sin\gamma}\delta y(k) \geq 1,\\
\textbf{b}\text{:}\quad & -\frac{\sin(\varphi(k)-\gamma)}{(r_p-r_{tol})\sin\gamma}\delta x(k) + \frac{\cos(\varphi(k)-\gamma)}{(r_p-r_{tol})\sin\gamma}\delta y(k) \geq 1,\\
\textbf{c}\text{:}\quad & \frac{\cos\varphi(k)}{r_p\sin\gamma}\delta x(k) + \frac{\sin\varphi(k)}{r_p\sin\gamma}\delta y(k) \geq 1,
\end{aligned} \tag{10}$$

where $\varphi(k)$ is the angle between the platform docking port and the x-axis at the time instant k. When the docking port is not moving, $\varphi(k) = \varphi$, and the LOS constraints are linear inequalities in $\delta x(k)$ and $\delta y(k)$. For the case where the platform rotates we compare two approaches to the treatment of these constraints. In the first one, the constraints do not account for the predicted motion of the platform, i.e., $\varphi(k)$ is assumed to remain constant along the MPC prediction horizon. In the second approach the constraints along the prediction horizon account for the motion of the platform.

A. No prediction of platform motion

In the case of no prediction of platform motion, we set $\omega_p = 0$ and $\varphi(k) = \varphi$ in (6), (10), (9) hence resulting in

$$\bar{X}(k+1) = \bar{A}\bar{X}(k) + \bar{B}\bar{U}(k) \tag{11a}$$
$$\bar{Y}(k) = \bar{C}(k)\bar{X}(k) + \bar{D}\bar{U}(k) \tag{11b}$$

where (11b) represent the constrained outputs, i.e.,

$$\bar{Y}(k) \geq \bar{Y}_{min} \tag{12}$$

and $\bar{Y}_{min} = (\,1\ 1\ 1\ -\beta\,)^T$. By defining $\sigma = [\sigma_x\ \sigma_y]^T$, $\delta v = [\delta v_x\ \delta v_y]^T$, $\xi = [\sigma^T\ \delta v^T]^T$, the cost function of the MPC controller is formulated from P, Q, R in (3) as

$$\begin{aligned}
\bar{J} &= \bar{X}(N_J)^T\bar{P}\bar{X}(N_J) + \sum_{j=0}^{N_J-1}\bar{X}(j)^T\bar{Q}\bar{X}(j) + \bar{U}(j)^T\bar{R}\bar{U}(j)\\
&= \xi(N_J)^T P\xi(N_J)\\
&\quad + \sum_{j=0}^{N_J-1}\xi(j)^T Q\xi(j) + U(j)^T RU(j) + \rho s(j)^2.
\end{aligned} \tag{13}$$

Here $\rho > 0$ is a large weight on the slack variable causing this variable to be zero whenever feasible.

At every time instant k, the MPC controller solves

$$\begin{aligned}
\min_{\bar{\mathbf{U}}(k)}\ & \sum_{j=0}^{N_J-1}\bar{X}(j|k)^T\bar{Q}\bar{X}(j|k) + \bar{U}(j|k)^T\bar{R}\bar{U}(j|k)\\
& + \bar{X}(N_J|k)^T\bar{P}\bar{X}(N_J|k)\\
\text{s.t.}\ \ & \bar{X}(j+1|k) = \bar{A}\bar{X}(j|k) + \bar{B}\bar{U}(j|k)\\
& \bar{Y}(j|k) = \bar{C}(k)\bar{X}(j|k) + \bar{D}\bar{U}(j|k)\\
& \bar{Y}(j|k) \geq \bar{Y}_{min},\ j = 0,\dots,N_c\\
& \bar{U}(j|k) \geq \bar{U}_{min} j = 0,\dots,N_u\\
& \bar{U}(j|k) \leq \bar{U}_{max},\ j = 0,\dots,N_u\\
& \bar{X}(0|k) = \bar{X}(k)\\
& \bar{U}(j|k) = U(N_u|k),\ j = N_u,\dots N_J-1
\end{aligned} \tag{14}$$

where $a(j|k)$ indicates the value of a predicted j steps ahead from step k, $\bar{\mathbf{U}}(k) = \{\bar{U}_0, \bar{U}_1, \cdots, \bar{U}_{N_u}\}$, N_u denotes the control horizon, and N_c denotes the constraint horizon. The input constraints in (14) are formulated from (7). The first element of the optimizer of (14) is applied as input, i.e., $\bar{U}(k) = \bar{U}_{\mathrm{MPC}}(\bar{X}(k)) = \bar{U}_0^*(\bar{X}(k))$, where we highlight that the solution of (14) is function of $\bar{X}(k)$. Note also that due to $C(k)$, the constraints are time-varying, but they are assumed constant in the optimization problem (14).

B. Prediction of platform motion

Even if the constraints in (14) change with time, as the initial state of the finite horizon optimal control problem $X(k)$ changes, the bounds are assumed constant in prediction, i.e., $\varphi(k) = \varphi$, $\omega_p = 0$ are assumed in (14). In this section we propose a method to incorporate in the MPC optimization problem a prediction of the LOS constraint (10) changes due to the rotation of the docking port. In order to continue exploiting a linear-quadratic MPC framework, we employ the approximations

$$\varphi(h) \simeq \varphi(k) + \dot{\varphi}(k)(h-k)T_s = \varphi(k) + \bar{\varphi}(h,k,T_s) \tag{15}$$

$$\begin{aligned}
\sin(\varphi(h)+\gamma) &\simeq \sin(\varphi(k)+\gamma) + \cos(\varphi(k)+\gamma)\bar{\varphi}(h,k,T_s),\\
\cos(\varphi(h)+\gamma) &\simeq \cos(\varphi(k)+\gamma) - \sin(\varphi(k)+\gamma)\bar{\varphi}(h,k,T_s),
\end{aligned} \tag{16}$$

where k denotes the current time instant and $h \geq k$ is a future time instant. This results in the constraints

$$\begin{aligned}
\mathbf{a}'\text{:}\ & L_1\delta x(h) - L_2\delta(h)\\
& + \{L_2\delta x(k) + L_1\delta y(k)\}(\varphi(h) - \varphi(k)) \geq 1,\\
\mathbf{b}'\text{:}\ & -L_3\delta x(h) + L_4\delta y(h)\\
& - \{L_4\delta x(k) + L_3\delta y(k)\}(\varphi(h) - \varphi(k)) \geq 1,\\
\mathbf{c}'\text{:}\ & L_5\delta x(h) + L_6\delta y(h)\\
& - \{L_6\delta x(k) + L_5\delta y(k)\}(\varphi(h) - \varphi(k)) \geq 1,
\end{aligned} \tag{17}$$

where

$$L_1 = \frac{\sin(\varphi(k)+\gamma)}{(r_p-r_{tol})\sin\gamma}, L_2 = \frac{\cos(\varphi(k)+\gamma)}{(r_p-r_{tol})\sin\gamma},$$

$$L_3 = \frac{\sin(\varphi(k)-\gamma)}{(r_p-r_{tol})\sin\gamma}, L_4 = \frac{\cos(\varphi(k)-\gamma)}{(r_p-r_{tol})\sin\gamma},$$

$$L_5 = \frac{\cos(\varphi(k))}{r_p\sin\gamma}, L_6 = \frac{\sin(\varphi(k))}{r_p\sin\gamma}.$$

Introducing the auxiliary state variables

$$Z(k) = \begin{pmatrix} z_1 \\ z_2 \end{pmatrix} = \begin{pmatrix} \varphi(k+1) \\ \varphi(k) \end{pmatrix} = \begin{pmatrix} \varphi(k) + \omega_p T_s \\ \varphi(k) \end{pmatrix}, \tag{18}$$

it follows

$$Z(k+1) = \begin{pmatrix} 2 & -1 \\ 1 & 0 \end{pmatrix} Z(k) = \Theta Z(k). \tag{19}$$

Considering (6) (10), (9), (19), (9), (17) we obtain linear model with time-varying constraints

$$\tilde{X}(k+1) = \tilde{A}\tilde{X}(k) + \tilde{B}\tilde{U}(k) \tag{20a}$$
$$\tilde{Y}(k) = \tilde{C}(k)\tilde{X}(k) + \tilde{D}\tilde{U}(k) \tag{20b}$$

where $\tilde{U} = \bar{U}$, the state vector is

$$\tilde{X} = \begin{pmatrix} \delta x & \delta y & \delta\dot{x} & \delta\dot{y} & r_x & r_y & \sigma_x & \sigma_y & z_1 & z_2 \end{pmatrix}^T, \tag{21}$$

and the system constraints are

$$\tilde{Y}(k) \geq \tilde{Y}_{min}, \qquad \tilde{Y}_{min} = \bar{Y}_{min}. \tag{22}$$

The MPC cost function is defined as

$$\begin{aligned} \tilde{J} &= \tilde{X}(N_J)^T \tilde{P}\tilde{X}(N_J) + \sum_{j=0}^{N_J-1} \tilde{X}(j)^T \tilde{Q}\tilde{X}(j) + \tilde{U}(j)^T \tilde{R}\tilde{U}(j) \\ &= \xi(N_J)^T P \xi(N_J) \\ &\quad + \sum_{j=0}^{N_J-1} \xi(j)^T Q \xi(j) + U(j)^T R U(j) + \rho s(j)^2. \end{aligned} \tag{23}$$

From (20), (22), (23), (7) the MPC finite horizon optimal control problem with prediction of the LOS constraints dynamics is formulated similarly to (14).

IV. Simulated Maneuvers

We assume the following platform parameters: $r_p = 1.5$m, $\gamma = 30$deg, $r_{tol} = 0.1$m, $n = 1.107 \times 10^{-3}$rad/s (corresponding to the orbit of 500km above the Earth). The sampling period is $T_s = 0.5$s, and the simulations duration is 50s. In (8), we set $\eta = 0.5$ and $\beta = 0.1(1.5 + \omega_p)$ to relax the constraint in the case of a fast platform rotation. For MPC we select $N_J = 40$, $N_c = N_u = 5$. The input constraints of the spacecraft were set as $-0.8 \leq u_x \leq 0.8$, $-0.8 \leq u_y \leq 0.8$ (m/s^2).

In the first case study, the initial location for the spacecraft was $(\delta x_0, \delta y_0) = (50, -10)$ (in meters) and the initial position of the docking port was $(r_{x0}, r_{y_0}) = (1.5, 0)$ (in meters) which corresponded to radial approach, where the spacecraft approaches the platform along a radial line from the center of the Earth, if the platform were not rotating. With an aggressive platform rotation rate of $\omega_p = 5$deg/s the closed-loop responses without prediction of LOS constraint evolution due to platform motion, and with such a prediction are shown in Fig. 2 and Fig. 3, respectively. In both cases, the soft-docking, the LOS cone and thrust magnitude constraints are enforced by the MPC controller, and the spacecraft successfully completes the maneuver. Although relative velocity plots are not included in the paper due to lack of space, these confirm that the soft-docking constraints are satisfied

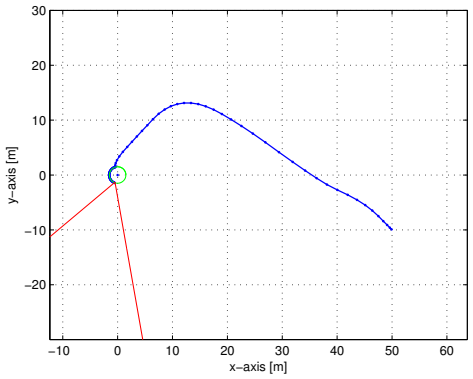

Fig. 2. Trajectory from radial approach without prediction of platform motion.

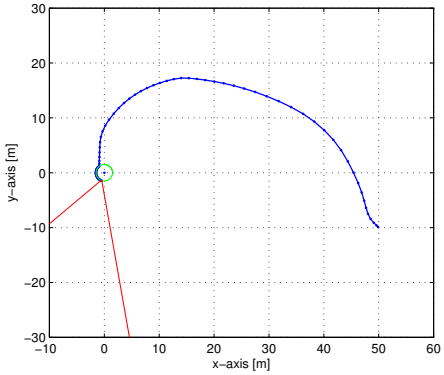

Fig. 3. Trajectory from radial approach with prediction of platform motion.

In the second case study, the initial location of the spacecraft is $(\delta x_0, \delta y_0) = (-10, 50)$ and the initial position of the docking port is $(r_{x0}, r_{y_0}) = (0, 1.5)$ which correspond to in-track approach where the spacecraft approaches the platform in a direction parallel to the orbit, if the platform was not rotating. With $\omega_p = 5$deg/s the closed-loop responses without prediction of LOS constraint evolution due to platform motion and with this prediction are shown in Fig. 4 and Fig. 5, respectively. Without prediction, the spacecraft fails the maneuver while with prediction the spacecraft is able to complete the maneuver while satisfying all the constraints.

The spacecraft trajectories starting from various initial locations within LOS cone are now examined for the case when the platform rotates with $\omega_p = 3$deg/s, see Fig. 6. With prediction of LOS motion, the spacecraft is able to successfully complete the maneuvers. Note that the trajectories initiated near the bottom of the LOS boundary require complicated spacecraft maneuvers to remain within the constraints. In the case of no prediction of LOS constraint motion, some maneuvers fail.

A. Fuel consumption analysis

We consider three performance metrics, $J_1 = \sum_{k=0}^{T_d} |u_x(k)| + |u_y(k)|$, $J_2 = \sum_{k=0}^{T_d} u_x(k)^2 + u_y(k)^2$, $J_3 = \sum_{k=0}^{T_d} \sqrt{(u_x(k))^2 + (u_y(k))^2}$, where $T_d = [t_d/T_s]$

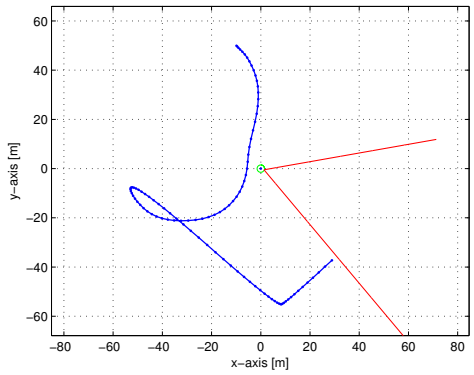

Fig. 4. Trajectory from in-track approach without prediction of platform motion. Docking fails.

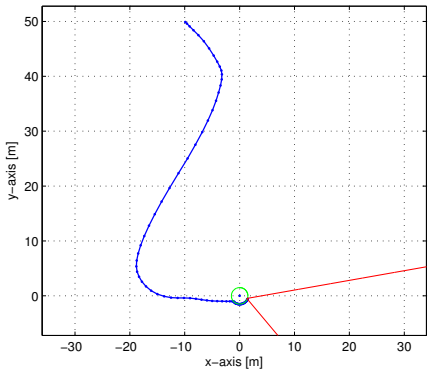

Fig. 5. Trajectory from in-track approach, with prediction of platform motion. Docking succeed.

and t_d is time to docking. While J_2 is related to the control effort penalty used in MPC, J_1 is related to the fuel consumption of a spacecraft which has two orthogonal families of pairs of thrusters, and J_3 is related to the fuel consumption of a spacecraft with a single thruster which is oriented as appropriate utilizing the attitude control.

Table I gives the results in the radial approach maneuver presented before, using $R = \alpha I$ – where the scalar α is varied – in (3). The three cost functions, J_1, J_2, J_3 appear to exhibit similar tendencies, justifying the use of J_2 to indirectly influence J_1 and J_3 when included as a part of MPC cost function. Note that when using prediction of the LOS dynamics the metrics are improved as compared to the case when the prediction is not used. These results suggest that including the prediction of the changes in the LOS constraint induced by the target platform rotating/tumbling motion is beneficial to obtain fuel-efficient maneuvers.

V. Debris Avoidance Maneuvers

In this section we consider the additional objective of avoiding a debris on the spacecraft rendezvous path. To simplify the problem the target platform is treated as a non-rotating point mass which is located at the origin. We "cover" the debris by a disk of radius r_d centered at (d_x, d_y).

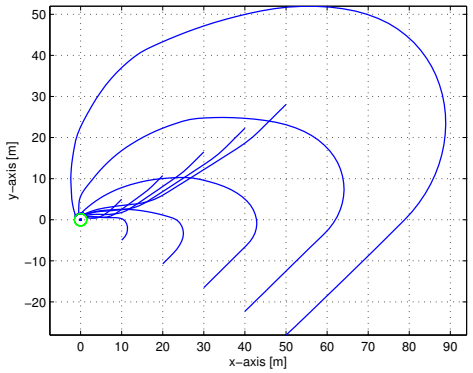

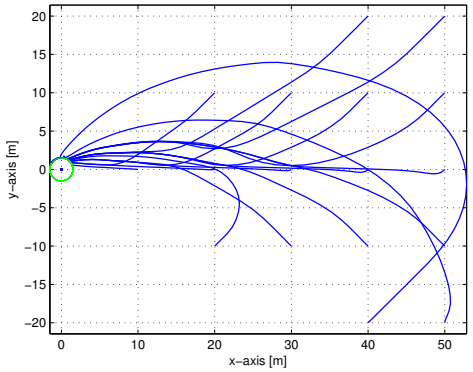

Fig. 6. Trajectories from different spacecraft initial locations: (top) from the LOS constraint boundaries; (bottom) from the interior of LOS constraints.

$\omega_p = 3$deg/s	α	10^7	10^8	5×10^8	10^9	5×10^9
no LOS pred.	J_1	37.51	28.42	33.43	36.13	40.66
	J_2	23.62	15.64	18.66	20.44	20.81
	J_3	28.20	22.71	25.83	27.74	30.53
	t_d	21.0	32.0	50.5	56.0	58.0
LOS pred.	J_1	28.63	25.89	21.86	20.97	19.88
	J_2	14.52	11.83	8.77	7.92	6.39
	J_3	21.62	20.94	17.53	16.86	16.19
	t_d	23.0	31.5	51.5	55.5	51.0

TABLE I

Fuel consumption related costs and docking time versus α.

For avoiding the debris we create a slow "virtual" rotation on the covering disk, with angular rate ω_d, and we impose that the spacecraft must remain in a specified half-plane relative to a tangent line to the disk, see Fig. 7. At activation, the disk tangent line is perpendicular to the line between the spacecraft location, $(\delta x(0), \delta y(0))$, and the center of the circle, (d_x, d_y). Then, $\varphi_d(0)$ is defined as the angle between the x-axis and the normal to the tangent line so that $\varphi_d(0) = \tan^{-1}\left(\frac{\delta y(0)-d_y}{\delta x(0)-d_x}\right)$, and $\varphi_d(k+1) = \varphi_d(k) + \omega_d T_s$. Thus, the debris avoidance constraint is formulated by

$$\frac{\cos\varphi_d(k)}{r_d}(\delta x(k) - d_x) + \frac{\sin\varphi_d(k)}{r_d}(\delta y(k) - d_y) \geq 1. \quad (24)$$

The approach developed in Section (III-B) is applied so

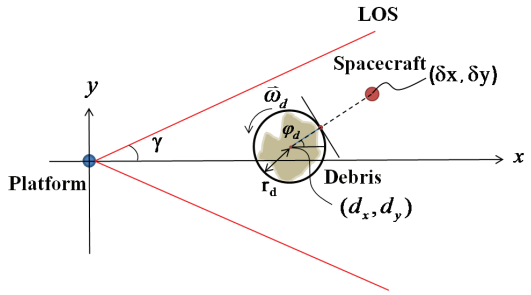

Fig. 7. Treating debris avoidance maneuvers.

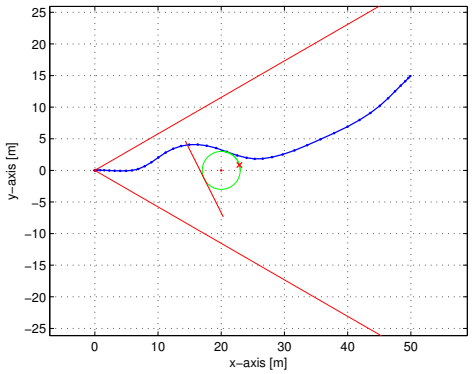

Fig. 8. Debris avoidance maneuver.

that (24) is approximated in prediction by

$$L_7(\delta x(h) - d_x) + L_8(\delta y(h) - d_y) + (-L_8(\delta x(k) - d_x) + L_7(\delta y(k) - d_y))(\varphi_d(h) - \varphi_d(k)) \geq 1, \quad (25)$$

where $L_7 = \frac{\cos\varphi_d(k_c)}{r_d}$, $L_8 = \frac{\sin\varphi_d(k_c)}{r_d}$ and

$$\varphi_d(h) \simeq \varphi_d(k) + \dot{\varphi}_d(k)(h-k)T_s.$$

The debris constraint is deactivated once φ_d becomes equal to $\varphi_d(0) + \pi$ so that the constraint does not interfere with the spacecraft motion after it passes the debris.

Thus, the model for the MPC finite horizon optimal control problem is defined by (6), (9), (10), (25), $d(k+1) = d(k)$, $d(k) = [d_x \ d_y]^T$, and by (19), where now $z_1(k) = \phi_d(k) + \omega_d T_s$, $z_2(k) = \phi_d(k)$. Constraint **c** is redundant in this case and is removed from (10), resulting in

$$\hat{X}(k+1) = \hat{A}\hat{X}(k) + \hat{B}\hat{U}(k), \quad (26a)$$

$$\hat{Y}(k) = \hat{C}(k)\hat{X}(k) + \hat{D}\hat{U}(k), \quad (26b)$$

where the state vector is

$$\hat{X} = \begin{pmatrix} \delta x & \delta y & \delta\dot{x} & \delta\dot{y} & d_x & d_y & r_x & r_y & z_{d_1} & z_{d_2} \end{pmatrix}^T$$

and where the constraint

$$\hat{Y}(k) \geq \hat{Y}_{min}, \ \hat{Y}_{min} = \begin{pmatrix} 1 & 1 & 1 & -\beta \end{pmatrix}^T \quad (27)$$

is imposed on the system output, representing the LOS constraints and the soft-landing constraints with respect to the platform, and the debris avoidance constraint.

The MPC problem cost function is

$$\hat{J} = \hat{X}(N_J)^T \hat{P}\hat{X}(N_J) + \sum_{j=0}^{N_J-1} \hat{X}(j)^T\hat{Q}\hat{X}(j) + \hat{U}(j)^T\hat{R}\hat{U}(j)$$
$$= \xi(N_J)^T P\xi(N_J) + \sum_{j=0}^{N_J-1} \xi(j)^T Q\xi(j) + U(j)^T RU(j) + \rho s(j)^2. \quad (28)$$

The finite horizon optimal control is formulated similarly to (14) using cost function (28), dynamics model (26), output constraints (27), and input constraints (7).

We have simulated the debris avoidance maneuver with $r_d = 3$m, and the other parameters as the ones in Section (IV). The debris is located at $(20, 0)$ (in meters) and the initial location for the spacecraft is at $(\delta x_0, \delta y_0) = (50, 15)$ (in meters). The docking port is located at the origin of the reference frame, and $\omega_d = 7$deg/s.

Fig. 8 compares the trajectory of the spacecraft when there is no debris and when the spacecraft performs a rendezvous while avoiding debris. The "x" symbol represents the initial point of activation of the tangent line constraint. The constraint is deactivated after the disk covering the debris has rotated π radians.

VI. Conclusions

In this paper we have examined the problem of spacecraft rendezvous and docking with a rotating/tumbling platform. Linear-quadratic Model Predictive Control (MPC) has been utilized to enforce thrust magnitude, LOS cone angle and velocity of approach (soft-docking) constraints. We have shown that predicting the motion of the docking port and the changes in the LOS constraints permits to satisfactory perform maneuvers initiated when the spacecraft is further away from the platform and when the platform is rotating at a higher rate. The prediction also helps to reduce the fuel consumption. Finally, we have demonstrated that closely related ideas can be used for debris avoidance during the rendezvous maneuver.

References

[1] L. Breger and J. How. Safe trajectories for autonomous rendezvous of spacecraft. *Journal of Guidance, Control, and Dynamics*, 31(5), 2008.

[2] W. Fehse. *Automated Rendezvous and Docking of Spacecraft.* Cambridge Aerospace Series, 2003.

[3] H. Park, S. Di Cairano and I. Kolmanovsky. Model Predictive Control of spacecraft docking with a non-rotating platform. *18th IFAC World Congress*, 2011, to appear.

[4] A. Richards and J. How. Performance evaluation of rendezvous using model predictive control. *AIAA Guidance, Navigation, and Control Conference and Exhibit*, 2003.

[5] S. Di Cairano, I. Kolmanovsky, A. Bemporad and D. Hrovat. Model predictive control of magnetically actuated mass spring damper for automotive applications. *Int. J. Control*, 80(11):1701–1716, 2007.

[6] E. Hartley. *Model Predictive Control for Spacecraft Rendezvous*. Ph.D. Dissertation, University of Cambridge, UK, 2010.

[7] L. Singh, S. Bortolami and L. Page. Optimal guidance and thruster control in orbital approach and rendezvous for docking using model predictive control. *AIAA Guidance, Navigation, and Control Conf.*, AIAA 2010-7754, 2010.

[8] B. Wie. *Space Vehicle Dynamics and Control.* AIAA Education Series, 2008.